Cell Metabolism
Article

Fumarate Is Cardioprotective via Activation of the Nrf2 Antioxidant Pathway

Houman Ashrafian,[1,*] Gabor Czibik,[1,12] Mohamed Bellahcene,[1,12] Dunja Aksentijević,[1] Anthony C. Smith,[2] Sarah J. Mitchell,[3,4] Michael S. Dodd,[6] Jennifer Kirwan,[7] Jonathan J. Byrne,[7] Christian Ludwig,[8] Henrik Isackson,[1] Arash Yavari,[1] Nicolaj B. Støttrup,[9] Hussain Contractor,[1] Thomas J. Cahill,[1] Natasha Sahgal,[11] Daniel R. Ball,[6] Rune I.D. Birkler,[9] Iain Hargreaves,[10] Daniel A. Tennant,[8] John Land,[10] Craig A. Lygate,[1] Mogens Johannsen,[9] Rajesh K. Kharbanda,[1] Stefan Neubauer,[1] Charles Redwood,[1] Rafael de Cabo,[4] Ismayil Ahmet,[5] Mark Talan,[5] Ulrich L. Günther,[8] Alan J. Robinson,[2] Mark R. Viant,[7] Patrick J. Pollard,[10] Damian J. Tyler,[6] and Hugh Watkins[1,11]
[1]Department of Cardiovascular Medicine, University of Oxford, Oxford OX3 9DU, UK
[2]Medical Research Council Mitochondrial Biology Unit, Cambridge CB2 0XY, UK
[3]Kolling Institute of Medical Research, Royal North Shore Hospital, University of Sydney, Sydney NSW 2065, Australia
[4]Laboratory of Experimental Gerontology
[5]Laboratory of Cardiovascular Science
National Institute on Aging, National Institutes of Health, Baltimore, MD 21224-6825, USA
[6]Cardiac Metabolism Research Group, Department of Physiology, Anatomy, and Genetics, University of Oxford, Oxford OX1 3QX, UK
[7]School of Biosciences
[8]School of Cancer Sciences
University of Birmingham, Birmingham B15 2TT, UK
[9]Department of Cardiology, Skejby Hospital, and Section for Toxicology and Drug Analysis, Department of Forensic Medicine, Aarhus University Hospital, Aarhus N 8200, Denmark
[10]Neurometabolic Unit, National Hospital of Neurology, London WC1N 3BG, UK
[11]Nuffield Department of Medicine, Henry Wellcome Building for Molecular Physiology, University of Oxford, Oxford OX3 7BN, UK
[12]These authors contributed equally to this work
*Correspondence: houman.ashrafian@cardiov.ox.ac.uk
DOI 10.1016/j.cmet.2012.01.017

SUMMARY

The citric acid cycle (CAC) metabolite fumarate has been proposed to be cardioprotective; however, its mechanisms of action remain to be determined. To augment cardiac fumarate levels and to assess fumarate's cardioprotective properties, we generated fumarate hydratase (*Fh1*) cardiac knockout (KO) mice. These fumarate-replete hearts were robustly protected from ischemia-reperfusion injury (I/R). To compensate for the loss of Fh1 activity, KO hearts maintain ATP levels in part by channeling amino acids into the CAC. In addition, by stabilizing the transcriptional regulator Nrf2, Fh1 KO hearts upregulate protective antioxidant response element genes. Supporting the importance of the latter mechanism, clinically relevant doses of dimethylfumarate upregulated Nrf2 and its target genes, hence protecting control hearts, but failed to similarly protect Nrf2-KO hearts in an in vivo model of myocardial infarction. We propose that clinically established fumarate derivatives activate the Nrf2 pathway and are readily testable cytoprotective agents.

INTRODUCTION

The observation that exposing hearts to brief, repeated episodes of ischemia renders them resistant to the sequelae of prolonged I/R has triggered the search for pharmacological agents, including metabolic agents, that recapitulate this cardioprotection (Yellon and Hausenloy, 2007). Although the literature relating metabolism to cardioprotection is dominated by accounts of carbohydrate metabolism (Howell et al., 2011), other metabolites, such as amino acids and citric acid cycle (CAC) intermediates, also contribute to the myocardial response to ischemia. Previous studies have reported that the hypoxic/ischemic myocardium converts aspartate and glutamate to succinate via the CAC (Figure 1), yielding ATP and GTP (Hochachka et al., 1975; Taegtmeyer, 1978; Sanborn et al., 1979; Hohl et al., 1987). This channeling of amino acids through the CAC has been proposed to be beneficial by virtue of its capacity to maintain redox potentials and to yield high-energy phosphates. However, despite the plausibility of these pathways (Penney and Cascarano, 1970), their contribution to I/R and cardioprotection in the mammalian heart remains contentious (Sanborn et al., 1979; Peuhkurinen et al., 1983; Hohl et al., 1987; Wiesner et al., 1988; Penney and Cascarano, 1970).

Recognizing the central role of fumarate to the above pathway, Des Rosiers and colleagues studied metabolic fluxes in fumarate-perfused rat hearts (Laplante et al., 1997). While this study substantiated the potentially cardioprotective influence of exogenous fumarate, it raised a number of questions. As the kinetic characteristics of the mammalian dicarboxylate transporter are poorly understood (Gallagher et al., 2009), the 0.04–0.4 mM of fumarate in the perfusate may not have optimally raised intracellular fumarate levels, resulting in relatively modest cardioprotection. Moreover, since the yield of ATP directly derived from fumarate metabolism was 100-fold lower than the rate of lactate

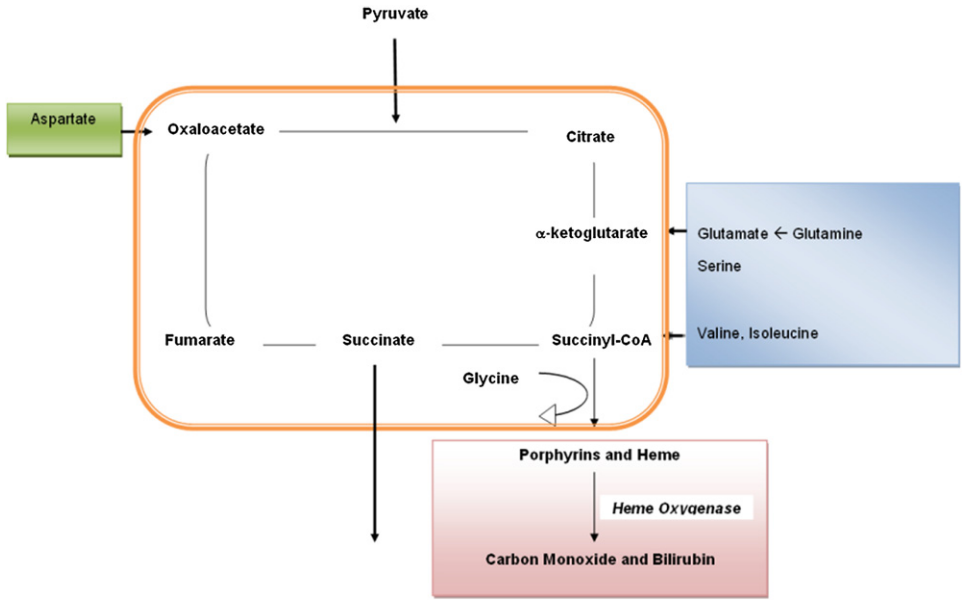

Figure 1. A Summary of Metabolic Pathways Relating to the CAC

Carbons derived from amino acids contribute to citric acid cycle (CAC) flux (anaplerosis), reducing NAD+ to NADH and ultimately yielding ATP. To maintain this energy-yielding flow, especially in the context of CAC interruption and during hypoxia/ischemia, carbon moieties must exit the CAC, e.g., through succinate and succinyl CoA.

release, the invocation of additional mechanisms was necessary to account for fumarate's cardioprotective properties (Penney and Cascarano, 1970; Peuhkurinen et al., 1983). These included fumarate's putative capacity to preserve cellular redox potential, improve calcium homeostasis, decrease free radical production, and reduce toxic acyl-CoA derivative accumulation during I/R (Laplante et al., 1997).

To increase myocardial fumarate concentrations and to permit delineation of the mechanisms through which fumarate might confer cardioprotection, we began by generating a mouse model of fumarate augmentation. We used a gene-targeted mouse with *loxP* sequences flanking exons 2 and 3 of the fumarate hydratase gene (*Fh1*)—$Fh11^{fl/fl}$ (Pollard et al., 2007). Inactivation of Fh11 in the kidney achieved by crossing $Fh11^{fl/fl}$ mice with mice expressing Cre recombinase under the Ksp-cadherin promoter (Ksp1.3/Cre) resulted in healthy animals despite substantially increased fumarate concentrations (Pollard et al., 2007; Ashrafian et al., 2010). Reassured by this unexpectedly mild phenotype, we similarly inactivated cardiac *Fh11* (specifically in cardiomyocytes) by breeding $Fh11^{fl/fl}$ mice with mice expressing Cre recombinase under the cardiomyocyte-specific promoter of myosin light chain—(MLC2v)-Cre (Chen et al., 1998). We sought to (1) assess whether cardiac function is maintained despite Fh1 inactivation in $Fh11^{fl/fl}$ MLC2v-Cre hearts and whether they exhibit increased fumarate levels, (2) determine whether these hearts are protected against I/R, (3) investigate the metabolic and other mechanisms of cardioprotection, and finally (4) ascertain whether any of the beneficial effects are directly attributable to fumarate by assessing the cardioprotective effects of exogenous oral fumaric acid derivatives (FADs) in nontransgenic animals experiencing I/R in vivo.

RESULTS

Cardiac Structure and Function Are Comparable in Fh1 Knockout and Control Mice

To understand the consequences of cardiac fumarate augmentation $Fh1^{fl/fl}$ MLC2v-Cre (termed Fh1 KO) (Figure 2A), $Fh1^{fl/+}$ MLC2v-Cre and $Fh1^{fl/fl}$ (termed controls and indistinguishable from wild-type [WT] controls) were observed to be healthy until ~3 months of age, when they develop ventricular dysfunction—the metabolic and redox basis of which is the subject of ongoing investigation. Experiments were therefore performed in ~6-week-old mice. Immunoblotting confirmed depletion of Fh1 protein in Fh1 KO mice compared to controls (29% ± 8% versus 100% ± 16%; $p < 0.05$) (Figure 2B). The remaining protein reflects persisting Fh1 in the nonmyocyte compartment (in which Cre is not expressed), as Fh1 transcript and protein are almost completely absent from isolated Fh1 KO cardiomyocytes (Figure 2C). Substantial metabolic differences exist between the Fh1 KO and control mice (see Figure S2 and Table S1 online), including a significant increase in whole-heart fumarate levels in Fh1 KO animals as derived from 1D ^{1}H NMR spectroscopy (Fh1 KO:control ratio, 1.63:1; $p < 0.005$). Despite the Fh1 depletion, cardiac structure and function including myocyte size (Figure 2D), heart weight:body weight ratio (Figure 2E), and ejection fraction (Figure 2F), as well as function assessed by cine MRI (data not shown), were similar in young Fh1 KO and controls. Heart rate, blood pressure (Figure 2G), and comprehensive assessment of LV function in vivo were comparable between both groups. The only difference was in the LV end-diastolic pressure, which decreased greater with dobutamine in Fh1 KO compared to controls (at baseline, 5.61 ± 1.52 versus 10.06 ± 3.74; after

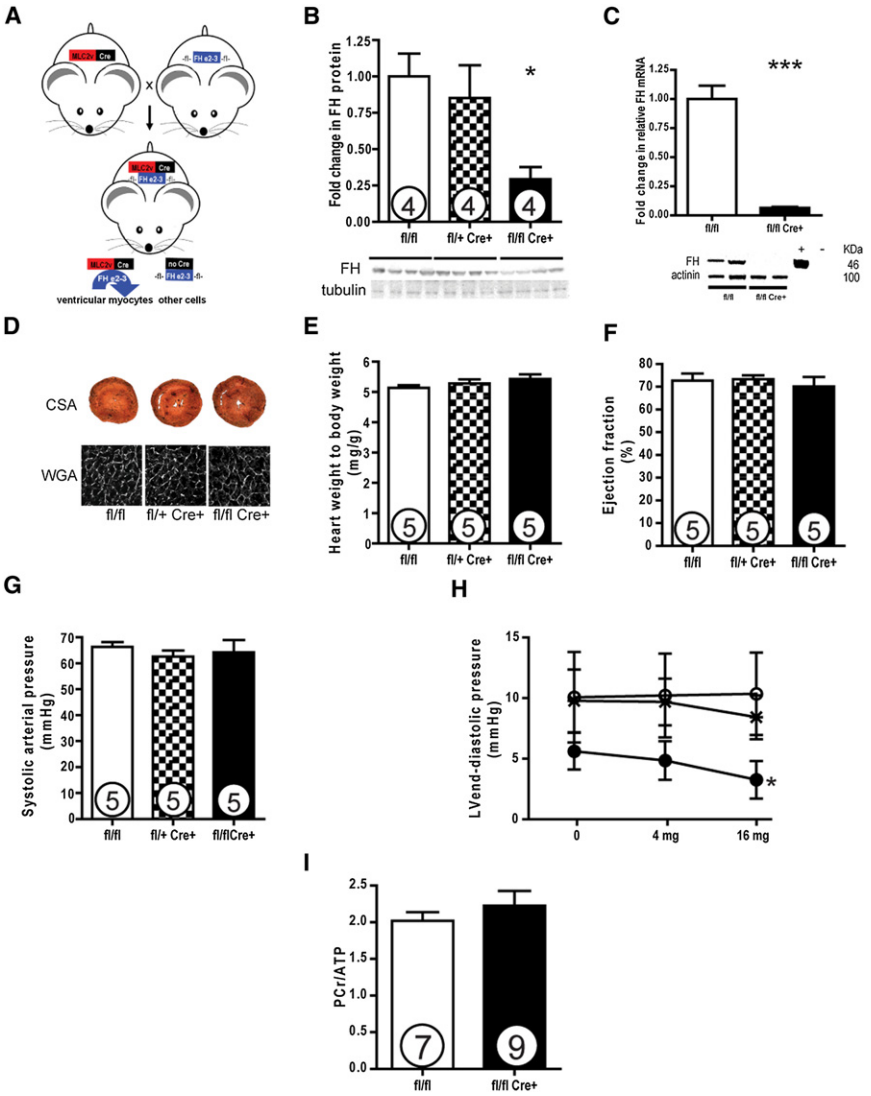

Figure 2. Fh1 KO Hearts Are Anatomically and Physiologically Comparable to Controls

(A) *Fh1*$^{fl/fl}$ mice (Pollard et al., 2007) were crossed with mice expressing Cre recombinase under the promoter of myosin light chain, (MLC2v)-Cre (Chen et al., 1998), to generate heterozygous and homozygous knockout (KO) mice.

(B) Assessed at 5–6 weeks of age, Fh1 KO hearts had substantially reduced Fh1 protein levels as demonstrated by the representative immunoblots and densitometric analysis (29% of controls).

(C) Isolated cardiomyocytes in Fh1 KO had complete depletion of Fh1 protein.

(D and E) Fh1 KO hearts were comparable to controls, with no evidence of cellular hypertrophy as assessed by wheat germ agglutinin (WGA) and gross hypertrophy.

(F) Systolic cardiac function as assessed by echocardiographic left ventricular ejection fraction was comparable between KO and control hearts.

(G and H) Invasive assessment of blood pressure and of contractile function revealed that Fh1 KO hearts were comparable to controls except with respect to LVEDP (H), which decreased in Fh1 KO hearts with increasing doses of dobutamine. ○, controls; x, HET KO; ●, Fh1 KO.

(I) Fh1 KO hearts exhibited comparable baseline energetics to controls as assessed by ^{31}P-MRS. Values are mean ± SEM. *p < 0.05 versus *Fh1*$^{fl/fl}$ mice.

16 mg/kg dobutamine, 3.25 ± 1.55 versus 10.35 ± 3.41 mmHg; p < 0.05) (Figure 2H).

Energetics in Fh1 KO hearts were comparable to controls as assessed by ^{31}P-MRS measurement of the PCr:ATP ratio in perfused hearts (2.23 ± 0.20 versus 2.02 ± 0.12) (Figure 2I).

Fh1 KO Mice Are Protected from Ischemia-Reperfusion Injury

Using a perfused heart model of ischemia/reperfusion (I/R), we investigated the response of Fh1 KO and controls to global cardiac ischemia. We employed a relatively long (40 min) period of ischemia, as young hearts are more tolerant of ischemia (Willems et al., 2005)—shorter (30 min) periods of ischemia had similar effects (data not shown). The degree of necrosis expressed as percentage of total at risk myocardium (i.e., ventricular volume) was substantially decreased in the Fh1 KOs compared to controls (17% ± 4% versus 37% ± 5%; p < 0.005) (Figure 3A). The recovery of coronary flow (CF), an established surrogate for reduced I/R injury (Headrick et al., 2001), was increased in the Fh1 KO group compared to controls after reperfusion (mean CF, 2.4 ± 0.05 versus 1.7 ± 0.03 ml/min; ANOVA, p < 0.0001) (Figure 3B), consistent with reduced myocardial necrosis. This reduction in necrosis was corroborated by significantly reduced release of markers of myocardial injury including creatine kinase and cardiac troponin I (Figures 3C and 3D). The recovery of function, expressed as percentage of the initial rate pressure product, was not significantly different in Fh1 KO versus controls (97% ± 12% versus 78% ± 6%) (Figure 3E), a dissociation that has been recognized in cardioprotection (Cohen, 2004). Importantly, no differences were observed between Fh1 KO and controls in PCr, ATP, or P_i during the I/R protocol (data not shown).

Myocardial microdialysis was used to systematically profile the interstitial cardiac metabolite concentrations during the different phases of I/R. During ischemia, the concentrations of many CAC intermediates, as previously reported by the same technique, increased in both Fh1 KO and control hearts (Birkler et al., 2010). However, the concentrations of succinate and glutamate were lower in Fh1 KO hearts than in controls—a pattern that has previously been associated with reduced myocardial injury (Vincent et al., 2000; Liu et al., 2010). During ischemia, and in reperfusion, the interstitial purine concentrations increased. However, the adenosine levels were lower in Fh1 KO hearts compared to controls (Figures 3F–3K). This pattern of reduced purine metabolism, previously observed in

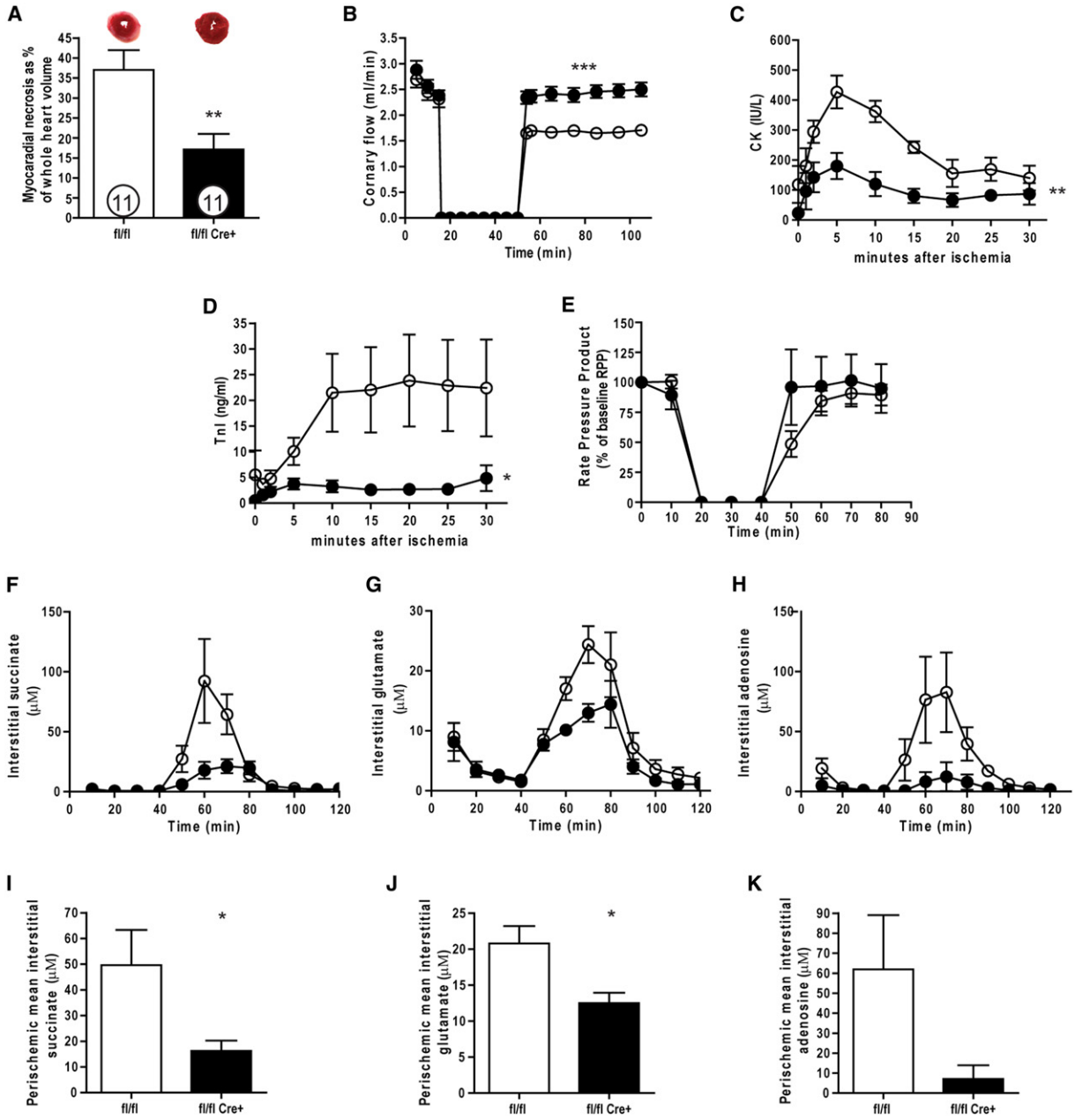

Figure 3. Cardiac Fh1 Deficiency Confers Cardioprotection

(A) Fh1-KO exhibited significant attenuation of myocardial necrosis (determined with TTC staining) compared with control hearts when perfused with 40 min of no-flow ischemia followed by 120 min of reperfusion.

(B) This was accompanied by substantially better recovery in coronary flow.

(C and D) This reduction in myocardial necrosis was confirmed by a significant reduction in markers of cardiac injury (cardiac troponin I, TnI; and creatine kinase, CK).

(E) Functional recovery as assessed by the rate pressure product was comparable in the Fh1-KOs and controls.

(F–K) Myocardial microdialysis coupled to an ultraperformance liquid chromatography/electrospray-tandem mass spectrometry approach demonstrated differences in the interstitial concentrations of succinate, glutamate, and adenosine during stabilization, ischemia, and reperfusion between Fh1-KO and control hearts. Fh1-KO (●) and controls (○). Values are mean ± SEM. *$p < 0.05$; **$p < 0.01$ versus control; ***$p < 0.001$ versus control.

ischemic preconditioning, is consistent with reduced myocardial injury and may indicate inhibition of adenine nucleotide catabolism resulting from the inhibition of 5′-nucleotidase activity (Van Wylen, 1994; Wikstrom et al., 1995).

Anaplerosis by Amino Acids Is a Prominent Adaptation to Fh1 Deletion

To determine the mechanisms of cardiac viability and I/R protection in hearts lacking Fh1, a critical component of the CAC, we

applied a flux balance analysis (FBA) model of mitochondrial metabolism to predict the consequences of Fh1 depletion (Smith and Robinson, 2011). The metabolic fluxes for maximal ATP production were determined on the basis of fixed reaction stoichiometry, reaction directionality accounting for thermodynamic requirements, protonation state differences between the cytosol and matrix, and known transport fluxes. This model predicted that deletion of Fh1, without any adaptations, disrupted flux around the CAC, causing a 96% drop in ATP production. However, increased import of glutamate, other amino acids, and metabolites related to the malate-aspartate shuttle restored cardiac NAD^+ reduction and ATP production (Figure 4A). In summary, a substantial anaplerotic amino acid flux into the CAC is predicted to restore both spans of the CAC, maintaining [$NAD^+ \rightarrow$NADH], oxidative phosphorylation, and energetic viability. 1D ^{1}H NMR confirmed the perturbation of many of the metabolites identified in our in silico analysis (Table 1). Although this steady-state metabolomics is a metabolic snapshot supporting our predictions, inferences about metabolic fluxes are necessarily limited.

To investigate our metabolic model further, we studied Fh1 KO cardiac metabolism in vivo with hyperpolarized magnetic resonance spectroscopy using [1-^{13}C]pyruvate and [2-^{13}C]pyruvate to measure the rate of glycolytic (i.e., pyruvate dehydrogenase [Pdh] fluxes and lactate dehydrogenase [Ldh]) and CAC fluxes, respectively (Schroeder et al., 2008, 2009). Although Fh1 KO hearts manifest increased steady-state lactate levels (Fh1 KO, control ratio 1.26:1; $p = 0.034$) (Table 1), consistent with increased glycolysis in Fh1 KO hearts as in other tissues (Ashrafian et al., 2010), no pyruvate flux differences were apparent between Fh1 KO and control hearts (Figure S4). Finally, to determine the influence of Fh1 deletion on the metabolic fate of amino acids, we perfused Fh1 KO and controls hearts ex vivo with [3-^{13}C]glutamate with subsequent 2D 13C-HSQC NMR analysis. As expected, fumarate levels were significantly higher in Fh1 KO hearts. Moreover, supporting the proposal that Fh1 KO hearts augment amino acid derived flux through the CAC, we observed significantly increased label incorporation into CAC metabolites (e.g., aspartate and pyruvate [at C2 and C3], likely by reductive carboxylation) in Fh1 KO hearts compared to controls (Figure S5).

Supporting these observations, the expression of mRNA coding for glycolytic enzymes, biochemical measures of glycolytic enzyme activity, mitochondrial respiratory chain complex activity, and myofiber oxygen consumption showed no differences between Fh1 KO and control hearts (Figure S6). Overall, these metabolic studies reinforce the role of increased amino acid metabolism as an important mechanism contributing to the maintenance of CAC activity and hence viability in Fh1 KO hearts.

Fh1 KO Hearts Activate the Nrf2 Pathway that Mediates Cardioprotection

To identify signaling pathways that contribute to cardioprotection, we used microarray analysis (Table S2) with qRT-PCR validation of Fh1 KO and control heart mRNA. Canonical Nrf2 target genes (Kwak et al., 2003; Hayes et al., 2010) and coregulated genes encoding antioxidant enzymes of one-carbon metabolism (Harding et al., 2003) showed prominent differential expression between Fh1 KO and controls (fold change KO:control is as follows: *Hmox1*, 1.5× ± 0.1×, $p < 0.01$; *Nqo1*, 1.9× ± 0.2x×, $p < 0.01$; *Mthfd2*, 24× ± 4×, $p < 0.001$; *Gsta1*, 173× ± 49×, $p < 0.001$) (Figure 4B). To assess if this increase in Nrf2-dependent target genes resulted from a stabilization of Nrf2 protein related to modification of its inhibitor—Kelch-like ECH-associated protein 1 (Keap1)—immunoblotting was performed. This confirmed downregulation of Keap1 protein (fold change KO:control, 0.66× ± 0.05×, $p < 0.01$; despite unchanged Keap1 mRNA expression levels, Figure S1) and upregulation of Nrf2 (1.99× ± 0.58×, $p < 0.05$), Hmox1 (2.73× ± 0.71×, $p < 0.05$), Nqo1 (2.24× ± 0.42×, $p < 0.05$), Mthfd2 (19.91× ± 5.94×, $p < 0.05$), Gsta3 (1.7× ± 0.34×, $p < 0.05$), and Gsta1 (149.0× ± 43.7×, $p < 0.05$) proteins, which corresponded well to the gene expression changes (Figure 4C). To assess whether the pseudohypoxic properties of fumarate or succinate resulted in HIF-1α stabilization in this model (Ashrafian et al., 2010), qRT-PCR was used to quantify a panel of HIF targets—these were not raised in Fh1 KO hearts (Figure S1).

Both endogenous (i.e., Fh1 KO) and exogenous fumarate augmentation in cells have been reported to modify and inactivate Keap1 by modification at cysteines 151 and 288 in vitro (Linker et al., 2011; Adam et al., 2011; Ooi et al., 2011). To address whether this "succination" was pertinent to Fh1 KO hearts in vivo, whole-cell lysates from Fh1 KO and control hearts were probed with an antibody to S-(2-succinyl)cysteine (2SC) (Blatnik et al., 2008; Bardella et al., 2011). Fh1 KO hearts had increased levels of 2SC compared to controls (2.49×, $p < 0.001$) (Figure 4D). These findings, coupled with Keap1's sensitivity to electrophiles (Taguchi et al., 2011), support the proposal that Keap1 succination in Fh1 KO hearts is the cause of Nrf2 activation (Adam et al., 2011; Ooi et al., 2011).

One transcriptional consequence of Fh1 deficiency is Hmox1 upregulation. Since Hmox1 is cardioprotective (Melo et al., 2002; Piantadosi et al., 2008; Soares et al., 1998; Yet et al., 2001), we hypothesized that Hmox1 contributed to fumarate-related cardioprotection and assessed the effect of zinc deuteroporphyrin 2,4-bis glycol (ZnBG), a well-established and relatively specific Hmox1 inhibitor (Vreman et al., 1991; Appleton et al., 1999; Zhang et al., 2002; Morioka et al., 2006; Czibik et al., 2009). Inhibition of Hmox1 by ZnBG abrogated cardioprotection in the Fh1 KO hearts (33.3% ± 2.2% control; 11.4% ± 1.5% Fh1 KO; 30.1% ± 2.7% control + ZnBG; 35.2% ± 4.6% Fh1 KO + ZnBG; Fh1 KO ANOVA $p < 0.001$ versus all other groups) (Figure 4E).

Exogenous Fumarate Is Protective against Cardiac Ischemia-Reperfusion Injury

To investigate whether our observations in our Fh1 KO model are directly attributable to elevated fumarate and amenable to clinical translation, we assessed the consequences of fumarate augmentation. Mice were gavaged with dimethylfumarate (DMF) 15 mg/kg twice daily (comparable to a dose well-tolerated by humans and applicable to clinical practice) for 5 days (Linker et al., 2011; Kappos et al., 2008). We found that, compared with the vehicle-treated controls, DMF stabilized and increased Nrf2 protein (1.48× ± 0.15×, $p < 0.05$). Further, using confocal immunofluorescence microscopy, we were also able to demonstrate that low concentrations of DMF (10 μM) promoted Nrf2 nuclear translocation in cardiomyocyte-like HL-1 cells (Figure 5A).

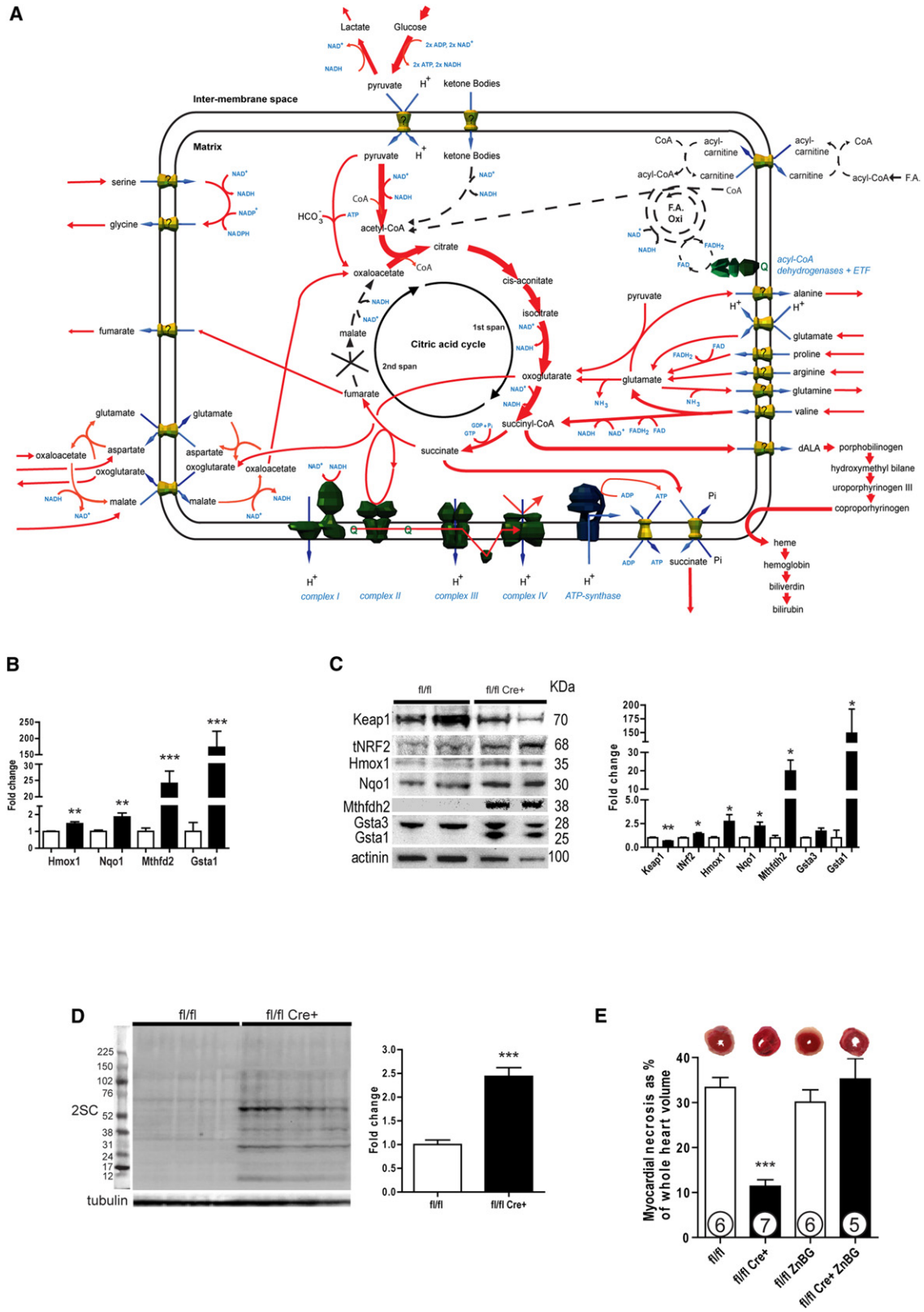

Figure 4. Fh1 Deficiency Confers Cardioprotection through Both Increasing Carbon Flux and Upregulating Heme Oxygenase 1 by Nrf2

(A) In silico modeling of optimal metabolic flux distributions for maximal ATP production in Fh1-deficient hearts. In contrast to the normal heart (Figure S3), reconstituting the CAC around absent Fh1 requires amino acids (e.g., glutamate and branched chain amino acids) to be fed into the first span of the CAC and

Table 1. 1D ^{1}H NMR Analysis Results Comparing the Metabolite Profiles of Fh1 KO against Control Hearts

Metabolite	Fold Change, *Fh1*$^{-/-}$ versus WT	T Test p
3-Hydroxybutyrate	1.844	0.0030
Alanine	1.230	0.0286
Fumarate	1.634	0.0044
Glutamate	0.829	0.0109
Glycine	1.153	0.0328
Isoleucine	1.298	0.0087
Lactate	1.26	0.034
Serine	1.288	0.0153
Succinate	1.817	6.72E-06
Taurine	0.893	0.0142
Valine	1.327	0.0002

DMF-treated mice recapitulated much of the cardiac Nrf2-dependent transcriptional profile noted in Fh1 KO mice (*Hmox1*, 1.6× ± 0.1×, $p < 0.05$; *Nqo1*, 2.8× ± 0.6×, $p < 0.05$; *Mthfd2*, 1.1× ± 0.1×, ns; *Gsta1*, 12.9× ± 3.5×, $p < 0.01$) (Figure 5B), which translated to proteins as assessed by immunoblotting: Hmox1 (2.40× ± 0.27×, $p < 0.0001$), Nqo1 (3.09× ± 0.33×, $p < 0.0001$), Gsta3 (3.11× ± 0.18×, $p < 0.0001$), and Gsta1 (6.27× ± 0.43×, $p < 0.0001$) (Figure 5C). Consistent with our observations in the Fh1 KO hearts, DMF-treated animals showed profoundly reduced myocardial necrosis when compared to vehicle in the perfused heart model (9.3% ± 1.2% versus 36.9% ± 3.9%, respectively; $p < 0.0001$) (Figure 5D) and resulted in a more rapid recovery of coronary flow (mean CF, 1.9 ± 0.05 versus 1.6 ± 0.04 ml/min; two-way ANOVA, $p < 0.05$) (Figure 5E). Finally, to assess the consequences of Nrf2 deletion on cardioprotection by DMF in vivo, 4-month-old WT and Nrf2 knockout (Nrf2 KO) mice after oral DMF or vehicle treatment underwent a coronary artery ligation model of myocardial infarction (MI). DMF significantly reduced the size of the MI/area at risk in WT mice compared to vehicle-treated WT controls ($p < 0.05$ by ANOVA with Bonferroni post hoc correction), but not in the DMF-treated Nrf2 KO mice compared to vehicle-treated Nrf2 KO controls (44.6% ± 3.9% versus 62.2% ± 3.9% and 63% ± 4.1% versus 57.9% ± 3.8%, respectively; $p < 0.001$ by ANOVA), affirming the importance of Nrf2 to fumarate-related cardioprotection (Figure 5F).

DISCUSSION

There is an increasing recognition that metabolites (e.g., succinate), in addition to their roles in generating energy through intermediary metabolism, have an important role in sensing and marshalling responses to diverse cellular stresses including I/R injury (Sapieha et al., 2008). Accordingly, the present study demonstrates that augmentation of myocardial fumarate, whether through Fh1 depletion or by DMF treatment, is cardioprotective. Predictions from an in silico model of the mitochondrial metabolome suggest that augmented anaplerotic channeling of carbon moieties from amino acids into the CAC contributes to the viability of Fh1-deficient hearts. These metabolic adaptations, coupled with fumarate-related upregulation of an Nrf2 antioxidant response—a response substantially recapitulated by DMF—result in cardioprotection.

The surprisingly mild phenotype of renal (Pollard et al., 2007) and cardiac Fh1 deficiency (despite an incomplete CAC) is not easily explained by our current knowledge. In order to discern the consequences of such metabolic perturbations, we used a FBA model of metabolism to simulate the effect of Fh1 deletion (Smith and Robinson, 2011). These simulations suggest that as compensation for Fh1 depletion, there is substantial metabolic remodeling, with likely carbon influx into the CAC from glutamate/glutamine, aspartate, and branched chain amino acids that reconstitutes and maintains oxidative flux. As a corollary, our in vivo metabolic imaging (Schroeder et al., 2008, 2009), biochemical measures of glycolysis, mitochondrial electron chain complex activity, and myofiber oxygen consumption studies confirm that Fh1 KO hearts largely maintain oxidative metabolism. Our observation of increased steady-state lactate levels in Fh1 KO hearts also raises the possibility of increased glycolytic flux through LDH in Fh1 KO hearts. However, our in vivo assessment of LDH and PDH fluxes by [1-^{13}C]pyruvate and [2-^{13}C]pyruvate, that might have been expected to show increased LDH exchange flux in the context of increased steady-state lactate, increased LDH activity, and/or increased NADH:NAD+, did not confirm such an increased LDH flux (Witney et al., 2011). Nonetheless, the application of complimentary techniques, including in vivo 18-fluorodeoxyglucose PET or ex vivo perfusion with labeled glucose, along with measures of lactate production, especially during stress, are needed to confirm this observation. One mechanism contributing to the maintenance of CAC activity, as predicted by the simulations, is increased amino acid-derived anaplerosis (the nonoxidative influx of metabolites into the CAC) as manifested by increased label incorporation into aspartate and pyruvate in Fh1 KO hearts perfused with [3-^{13}C]glutamate. While metabolic inferences from perfused hearts should be related to in vivo cardiac physiology cautiously (due to the unphysiological substrate profile and loading conditions used ex vivo), these observations underline the potential importance of amino acid flux to Fh1 KO hearts.

We also report that fumarate potently increased the expression of antioxidant response element (ARE)-regulated genes (e.g., *Gsta1*, *Nqo1*, and *Hmox1*) (Kwak et al., 2003; Hayes

aspartate, via the malate-asparate shuttle, into the second span of the CAC. This anaplerotic carbon flux is balanced by cataplerosis through succinate export and porphyrin synthesis-heme degradation channeled through Hmox1.
(B) Nrf2 target genes and the genes coding for the related antioxidant enzymes of one-carbon metabolism are significantly upregulated in Fh1-KO hearts as assessed by Taqman qRT-PCR. White bars, control; black bars, Fh1-KO.
(C) Representative immunoblots and densitometric analysis of Fh1-KO hearts demonstrating the downregulation of Keap1 and upregulation of Nrf2, Hmox1, Nqo1, Mthfdh2, Gsta3, and Gsta1.
(D) Fh1-KO hearts exhibit significantly increased levels of succination compared to WT.
(E) Hmox1 inhibition by ZnBG abrogates cardioprotection in Fh1-KO hearts as assessed by the extent of necrosis resulting from ex vivo cardiac I/R. Values are mean ± SEM. *$p < 0.05$; **$p < 0.01$; and ***$p < 0.001$ versus control.

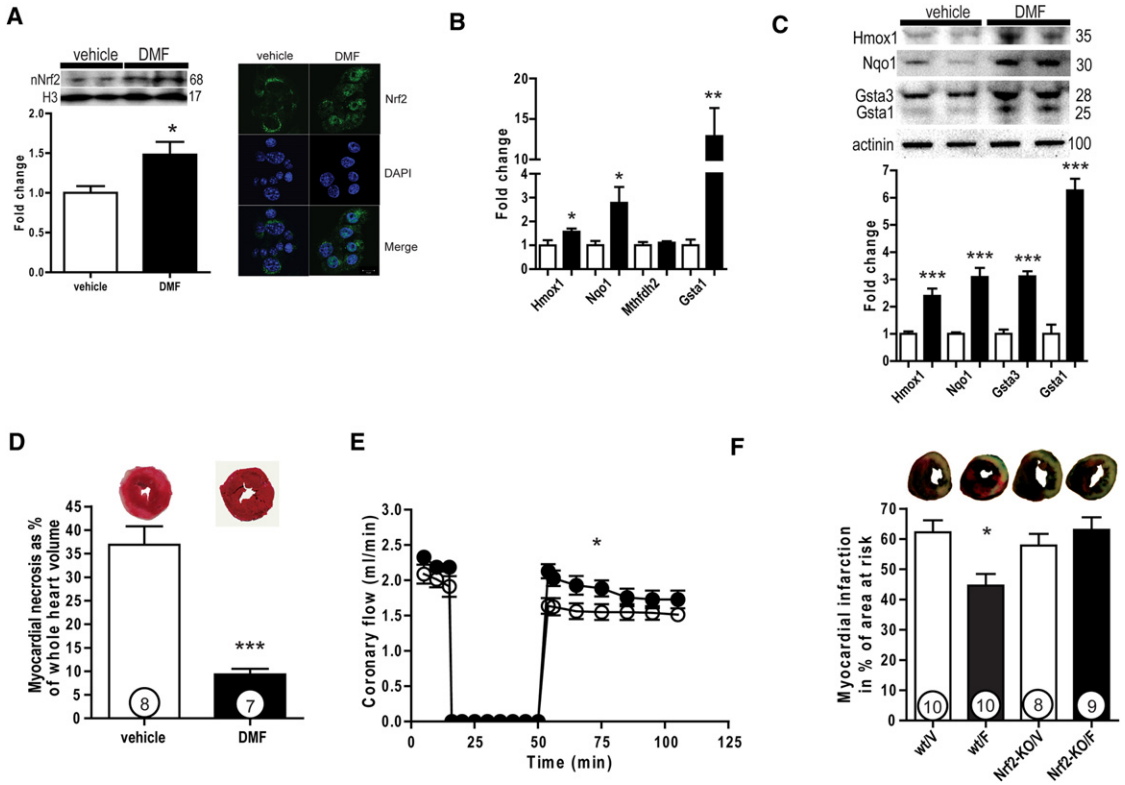

Figure 5. Administration of Fumarate Attenuates Ischemia-Reperfusion Injury

(A) Representative immunoblots and densitometric analysis of murine hearts gavaged with dimethylfumarate (DMF) at a dose of 15 mg/kg twice daily for 5 days, demonstrating the upregulation of Nrf2 (left). DMF (10 μM) for 6 hr promoted nuclear translocation and localization of Nrf2 in HL-1 cells as assessed by confocal microscopy (right).

(B) Oral DMF upregulates Nrf2 target genes as assessed by Taqman qPCR.

(C) Representative immunoblots (upper panel) and densitometric analysis (lower panel) of protein products of Nrf2 targets.

(D and E) Oral DMF treatment significantly attenuated myocardial necrosis resulting from ex vivo cardiac I/R and (E) was accompanied by an improved recovery in coronary flow.

(F) To assess the cardioprotective effect of fumarate in vivo and the pertinence of Nrf2 to this protection, a coronary artery ligation model of acute MI was applied to WT and Nrf2-KO mice both treated with DMF and vehicle (n = 12 in each of the four groups). The average surgical mortality of coronary ligation surgery was 24% and did not differ significantly across the groups. WT and Nrf2-KO mice treated with vehicle (WT/V and Nrf2-KO/V, respectively) or 5 days of DMF (15 mg/kg) twice daily (WT/F and Nrf2-KO/F, respectively) via oral gavage as above. Representative sections of the myocardium from each group are presented stained with 4% TTC, with the necrotic area represented in white, the area at risk (AAR) in red, and the nonischemic area in blue. There was no significant difference in the size of the underperfused area (AAR/LV) for each group (data not shown). While DMF reduced MI size in the WT animals treated with DMF compared to vehicle-treated controls (MI/AAR by ANOVA with Bonferroni post hoc comparison to vehicle-treated WT mice), there was no difference in the MI size in Nrf2-KO-treated DMF and vehicle-treated control mice, nor was there a difference in MI size as a percentage of the LV area. Values are mean ± SEM. *$p < 0.05$; **$p < 0.01$; ***$p < 0.001$.

et al., 2010) through activation of the redox-sensitive transcription factor Nrf2 (Hayes and McMahon, 2009; Taguchi et al., 2011). In the Fh1 KO hearts, the coregulated enzymes of one carbon metabolism (e.g., *Mthfd2*) were also raised (He et al., 2001; Harding et al., 2003; Adams, 2007; Afonyushkin et al., 2010; Lewerenz and Maher, 2011). Unstimulated, Nrf2 is sequestered by Keap1, promoting Nrf2 ubiquitination and degradation. During cell stress, Keap1, a cysteine-rich protein sensitive to oxidants/electrophiles, is modified on one or more of its functional cysteines (e.g., Cys^{151}, Cys^{288}, and Cys^{273}), releasing the sequestered Nrf2 and permitting Nrf2 to activate its target genes (Taguchi et al., 2011).

FADs are known to be biologically active electrophiles and inducers of glutathione transferases and NAD(P)H:quinone reductases (Spencer et al., 1990). Recently, FADs have been shown to modify Cys^{151} and Cys^{288} of Keap1 in vitro (Linker et al., 2011; Adam et al., 2011; Ooi et al., 2011). Although we were unable to immunoprecipitate sufficient protein in vivo from hearts to demonstrate Keap1 modification, using an antibody directed against (S-[2-succinyl] cysteine [2SC]) formed by a reaction between fumarate and cysteines in proteins (Blatnik et al., 2008), we demonstrated substantial 2SC modification in Fh1 KO hearts (Figure 3D). Similar fumarate-dependent succination has been observed in FH-deficient cells and HLRCC cancer tissue with corresponding Nrf2 stabilization (Bardella et al., 2011; Adam et al., 2011; Ooi et al., 2011). Thus, although we cannot exclude other Nrf2-stabilizing influences (Rada et al., 2011), given Keap1's sensitivity to electrophiles and its proximity to mitochondria (Lo and Hannink, 2008) (where fumarate concentrations are likely to be highest), coupled with increased

succination and the findings in FH-deficient cells (Adam et al., 2011; Ooi et al., 2011), we propose this represents strong, albeit circumstantial evidence that Keap1 is succinated in fumarate-replete hearts, explaining Nrf2 target gene upregulation by both Fh1 deletion and DMF treatment. That DMF promotes nuclear translocation of Nrf2 and that the protective properties of DMF are abolished in Nrf2-KO mice further support our proposal that Nrf2 has a central role in fumarate-related cardioprotection in vivo.

To reconcile the cardioprotection noted in young Fh1-deficient mice with the subsequent development of significant left ventricular dysfunction after 3 months of age, we propose that fumarate accumulation triggers both adaptive and maladaptive responses, respectively. While Nrf2 activation is known to be cardioprotective when acutely activated (Calvert et al., 2009; Motohashi and Yamamoto, 2004; Zhang et al., 2010), there is emerging evidence that chronic Nrf2 activation results in experimental and human cardiomyopathy (Rajasekaran et al., 2007, 2011). Thus, while Nrf2 activation by fumarate is beneficial in the context of ischemic stress, chronic Nrf2 activation is likely to be harmful and cause heart failure. A similarly biphasic pattern has been noted in animals with graded decrements in Keap1. While Keap1(flox/−) mice with increased Nrf2 levels are protected from the oxidative insults, a decrease in Keap1 levels to <50% results of controls increased long-term mortality (Taguchi et al., 2010).

A variety of interventions have been shown to reduce myocardial infarct size in animals; however, these interventions have translated poorly to man (Yellon and Hausenloy, 2007). While other Nrf2 inducers may be cardioprotective, including sulforaphane (found in broccoli) (Mukherjee et al., 2008), hydrogen sulphide (Calvert et al., 2009), and triterpenoid CDDO-imidazolide (Sussan et al., 2009), they lack human safety data, may be difficult to administer, and may have a low therapeutic index. In contrast, we demonstrate that oral FADs, which have already been successfully trialed in patients with psoriasis or multiple sclerosis (Kappos et al., 2008), are cytoprotective agents. This provides a strong rationale to investigate these safe and well-tolerated agents in clinical trials, for example to assess the impact of FADs in reducing myocardial injury in acute coronary syndromes or in patients undergoing predictable organ injury, e.g., surgery.

EXPERIMENTAL PROCEDURES

Mouse Husbandry

Procedures involving live animals were in accordance with UK Home Office guidelines and licensing regulations (project license 30/2444). MLC2v-cre mice were a kind gift from Professor Ken Chien (Chen et al., 1998). All mice were backcrossed onto a C57BL/6 genetic background for at least five generations. Male 4-month-old Nrf2 knockout (KO; n = 24) and WT (n = 24) mice, all on a CD-1 genetic background, were obtained from breeding colonies of the National Institute on Aging (Baltimore, MD). The mice were maintained on a 12 hr light/dark cycle with food and water available ad libitum. Experimental procedures were performed in accordance with the UK Home office and National Institutes of Health guidelines and approved by respective institutional review boards. In some experiments, Fh1 KO mice were treated with a specific heme oxygenase-1 inhibitor, ZnBG, once daily (30 mg/kg, i.p.) for 4 days prior to heart cannulation. For experiments investigating the role of oral FADs, C57Bl/6 mice (Harlan) were gavaged (15 mg/kg) twice daily for 5 days with dimethyl fumarate (DMF; Sigma) diluted in 0.08% methocel/H_2O before heart cannulation.

Cardiac Magnetic Resonance Scans, Cine

Animals were imaged using a standard cine MR imaging protocol (TR/TE, 4.6/1.755 ms; flip angle, 21°; averages, 4; slice thickness, 1.2 mm; matrix, 128 × 128; zero filled to 256 × 256; field of view, 51.2 × 51.2 mm). Scanning was performed on seven to eight contiguous slices in the short-axis orientation covering the entire heart. This was used to assess left ventricular mass and cardiac function in the 7 T MR scanner (Schroeder et al., 2008).

In Silico Analysis

Simulations were performed using the mitochondrial metabolic model iAS253 (Smith and Robinson, 2011) that was modified to include cytosolic reactions involved in the degradation of heme and an unconstrained boundary condition to allow the efflux of bilirubin. Additional constraints were applied to the fumarate and succinate inner mitochondrial membrane transport steps to represent restricted transport (especially for fumarate, as a specific mammalian fumarate transporter has not been identified). To determine the effect of increased metabolite uptakes on central metabolism, separate simulations were performed in which the allowable uptake range was increased. As uptake fluxes for metabolites were not available under perturbed conditions, these ranges were arbitrarily increased up to a maximum of 5 μmol/min/gDW. FBA was used to simulate the system using MATLAB (MathWorks, Inc., Natick, MA) and the COBRA toolbox in conjunction with the linear programming solver GLPK (http://www.gnu.org/software/glpk/). The resultant flux distributions were analyzed in Microsoft Excel and Cytoscape (Shannon et al., 2003).

Cardiac Magnetic Resonance Scans, Hyperpolarized ^{13}Cs

Hyperpolarized ^{13}C MRS Protocol [1-^{13}C]pyruvate or [2-^{13}C]pyruvate was hyperpolarized and dissolved as previously described. An aliquot of 0.2 ml of 80 mM hyperpolarized [1-^{13}C]pyruvate or [2-^{13}C]pyruvate solution was then injected over 10 s via a tail vein catheter into an anaesthetised mouse positioned in a 7 T MR scanner. Spectra were acquired for 1 min following injection with 1 s temporal resolution, and signal was localized to the heart using a home-built ^{13}C RF surface coil. Quantified peak areas were input into a kinetic model described by Atherton et al. (Atherton et al., 2011) and plotted against time in Microsoft Excel. This model fits the spectral peak areas as a function of time and accounts for several factors, including rate of injection, rate of signal decay for pyruvate and metabolites, and time of arrival for pyruvate and metabolites. This model determines the rate constant for pyruvate to metabolite exchange (kpyr-x, s-1), which is a measure of ^{13}C label incorporation into lactate, alanine, or bicarbonate pools.

Statistics

All data are expressed as mean ± standard error of the mean (SEM). Statistical analysis was performed using unpaired Student's t test or one-way ANOVA followed by the Bonferroni correction, where appropriate. Time course relationships were evaluated using two-way ANOVA. Statistical analysis was carried out using Graphpad Prism statistics software v.4. Differences were considered significant when $p < 0.05$.

Standard molecular and histologic methodology is described in the Supplemental Experimental Procedures.

SUPPLEMENTAL INFORMATION

Supplemental Information includes two tables, six figures, Supplemental Experimental Procedures, and Supplemental References and can be found with this article online at doi:10.1016/j.cmet.2012.01.017.

ACKNOWLEDGMENTS

H.A. and H.W. are supported by the Oxford British Heart Foundation Centre of Research Excellence Award, and the the British Heart Foundation (BHF Grant RG/02/010). A.J.R. and A.C.S. are supported by the Medical Research Council, UK. D.A. and S.N. are supported by the British Heart Foundation Programme Grant RG/05/005. M.S.D., D.R.B., and D.J.T. are supported by research grants from the British Heart Foundation, the Medical Research

Council, Oxford Instruments Molecular Biotools, and GE Healthcare. N.S.'s work is supported by the Core Award Grant 075491/Z/04 from the Wellcome Trust. N.B.S. is supported by the Fondation Leducq (06CVD) and the Lundbeck Foundation. P.J.P. is in receipt of a Beit Memorial Fellowship. S.J.M. is supported by a National Health and Medical Research Council of Australia CJ Martin Early Career Fellowship (1016439). The Thermo Scientific LTQ FT Ultra and Bruker NMR spectrometers used here were obtained through the Birmingham Science City Translational Medicine project, with support from Advantage West Midlands; the NMR spectrometer was further supported by the Wolfson Foundation. This study was also funded in part by the Intramural Research Program of the National Institute on Aging of the National Institutes of Health, USA. We gratefully acknowledge and thank Dr. Reza Morovat, consultant clinical biochemist at the Oxford Radcliffe NHS Trust, Oxford; and Dawn Phillips-Boyer and Dawn Nines for their excellent animal care and assistance.

Received: August 18, 2011
Revised: December 8, 2011
Accepted: January 18, 2012
Published online: March 6, 2012

REFERENCES

Adam, J., Hatipoglu, E., O'Flaherty, L., Ternette, N., Sahgal, N., Lockstone, H., Baban, D., Nye, E., Stamp, G.W., Wolhuter, K., et al. (2011). Renal cyst formation in Fh1-deficient mice is independent of the Hif/Phd pathway: roles for fumarate in KEAP1 succination and Nrf2 signaling. Cancer Cell *20*, 524–537.

Adams, C.M. (2007). Role of the transcription factor ATF4 in the anabolic actions of insulin and the anti-anabolic actions of glucocorticoids. J. Biol. Chem. *282*, 16744–16753.

Afonyushkin, T., Oskolkova, O.V., Philippova, M., Resink, T.J., Erne, P., Binder, B.R., and Bochkov, V.N. (2010). Oxidized phospholipids regulate expression of ATF4 and VEGF in endothelial cells via NRF2-dependent mechanism: novel point of convergence between electrophilic and unfolded protein stress pathways. Arterioscler. Thromb. Vasc. Biol. *30*, 1007–1013.

Appleton, S.D., Chretien, M.L., McLaughlin, B.E., Vreman, H.J., Stevenson, D.K., Brien, J.F., Nakatsu, K., Maurice, D.H., and Marks, G.S. (1999). Selective inhibition of heme oxygenase, without inhibition of nitric oxide synthase or soluble guanylyl cyclase, by metalloporphyrins at low concentrations. Drug Metab. Dispos. *27*, 1214–1219.

Ashrafian, H., O'Flaherty, L., Adam, J., Steeples, V., Chung, Y.L., East, P., Vanharanta, S., Lehtonen, H., Nye, E., Hatipoglu, E., et al. (2010). Expression profiling in progressive stages of fumarate-hydratase deficiency: the contribution of metabolic changes to tumorigenesis. Cancer Res. *70*, 9153–9165.

Atherton, H.J., Schroeder, M.A., Dodd, M.S., Heather, L.C., Carter, E.E., Cochlin, L.E., Nagel, S., Sibson, N.R., Radda, G.K., Clarke, K., and Tyler, D.J. (2011). Validation of the in vivo assessment of pyruvate dehydrogenase activity using hyperpolarised (13) C MRS. NMR Biomed. *24*, 201–208.

Bardella, C., El-Bahrawy, M., Frizzell, N., Adam, J., Ternette, N., Hatipoglu, E., Howarth, K., O'Flaherty, L., Roberts, I., Turner, G., et al. (2011). Aberrant succination of proteins in fumarate hydratase deficient mice and HLRCC patients is a robust biomarker of mutation status. J. Pathol. *224*, 1–10.

Birkler, R.I., Stottrup, N.B., Hermannson, S., Nielsen, T.T., Gregersen, N., Botker, H.E., Andreasen, M.F., and Johannsen, M. (2010). A UPLC-MS/MS application for profiling of intermediary energy metabolites in microdialysis samples—a method for high-throughput. J. Pharm. Biomed. Anal. *53*, 983–990.

Blatnik, M., Thorpe, S.R., and Baynes, J.W. (2008). Succination of proteins by fumarate: mechanism of inactivation of glyceraldehyde-3-phosphate dehydrogenase in diabetes. Ann. N Y Acad. Sci. *1126*, 272–275.

Calvert, J.W., Jha, S., Gundewar, S., Elrod, J.W., Ramachandran, A., Pattillo, C.B., Kevil, C.G., and Lefer, D.J. (2009). Hydrogen sulfide mediates cardioprotection through Nrf2 signaling. Circ. Res. *105*, 365–374.

Chen, J., Kubalak, S.W., and Chien, K.R. (1998). Ventricular muscle-restricted targeting of the RXRalpha gene reveals a non-cell-autonomous requirement in cardiac chamber morphogenesis. Development *125*, 1943–1949.

Cohen, M.V. (2004). Efficacy of preconditioning should be gauged by reduction of infarction. Br. J. Pharmacol. *141*, 197–198.

Czibik, G., Sagave, J., Martinov, V., Ishaq, B., Sohl, M., Sefland, I., Carlsen, H., Farnebo, F., Blomhoff, R., and Valen, G. (2009). Cardioprotection by hypoxia-inducible factor 1 alpha transfection in skeletal muscle is dependent on haem oxygenase activity in mice. Cardiovasc. Res. *82*, 107–114.

Gallagher, F.A., Kettunen, M.I., Hu, D.E., Jensen, P.R., Zandt, R.I., Karlsson, M., Gisselsson, A., Nelson, S.K., Witney, T.H., Bohndiek, S.E., et al. (2009). Production of hyperpolarized [1,4-13C2]malate from [1,4-13C2]fumarate is a marker of cell necrosis and treatment response in tumors. Proc. Natl. Acad. Sci. USA *106*, 19801–19806.

Harding, H.P., Zhang, Y., Zeng, H., Novoa, I., Lu, P.D., Calfon, M., Sadri, N., Yun, C., Popko, B., Paules, R., et al. (2003). An integrated stress response regulates amino acid metabolism and resistance to oxidative stress. Mol. Cell *11*, 619–633.

Hayes, J.D., and McMahon, M. (2009). NRF2 and KEAP1 mutations: permanent activation of an adaptive response in cancer. Trends Biochem. Sci. *34*, 176–188.

Hayes, J.D., McMahon, M., Chowdhry, S., and Dinkova-Kostova, A.T. (2010). Cancer chemoprevention mechanisms mediated through the Keap1-Nrf2 pathway. Antioxid. Redox Signal. *13*, 1713–1748.

He, C.H., Gong, P., Hu, B., Stewart, D., Choi, M.E., Choi, A.M., and Alam, J. (2001). Identification of activating transcription factor 4 (ATF4) as an Nrf2-interacting protein. Implication for heme oxygenase-1 gene regulation. J. Biol. Chem. *276*, 20858–20865.

Headrick, J.P., Peart, J., Hack, B., Flood, A., and Matherne, G.P. (2001). Functional properties and responses to ischaemia-reperfusion in Langendorff perfused mouse heart. Exp. Physiol. *86*, 703–716.

Hochachka, P.W., Owen, T.G., Allen, J.F., and Whittow, G.C. (1975). Multiple end products of anaerobiosis in diving vertebrates. Comp. Biochem. Physiol. B *50*, 17–22.

Hohl, C., Oestreich, R., Rosen, P., Wiesner, R., and Grieshaber, M. (1987). Evidence for succinate production by reduction of fumarate during hypoxia in isolated adult rat heart cells. Arch. Biochem. Biophys. *259*, 527–535.

Howell, N.J., Ashrafian, H., Drury, N.E., Ranasinghe, A.M., Contractor, H., Isackson, H., Calvert, M., Williams, L.K., Freemantle, N., Quinn, D.W., et al. (2011). Glucose-insulin-potassium reduces the incidence of low cardiac output episodes after aortic valve replacement for aortic stenosis in patients with left ventricular hypertrophy: results from the Hypertrophy, Insulin, Glucose, and Electrolytes (HINGE) trial. Circulation *123*, 170–177.

Kappos, L., Gold, R., Miller, D.H., Macmanus, D.G., Havrdova, E., Limmroth, V., Polman, C.H., Schmierer, K., Yousry, T.A., Yang, M., et al. (2008). Efficacy and safety of oral fumarate in patients with relapsing-remitting multiple sclerosis: a multicentre, randomised, double-blind, placebo-controlled phase IIb study. Lancet *372*, 1463–1472.

Kwak, M.K., Wakabayashi, N., Itoh, K., Motohashi, H., Yamamoto, M., and Kensler, T.W. (2003). Modulation of gene expression by cancer chemopreventive dithiolethiones through the Keap1-Nrf2 pathway. Identification of novel gene clusters for cell survival. J. Biol. Chem. *278*, 8135–8145.

Laplante, A., Vincent, G., Poirier, M., and Des, R.C. (1997). Effects and metabolism of fumarate in the perfused rat heart. A 13C mass isotopomer study. Am. J. Physiol. *272*, E74–E82.

Lewerenz, J., and Maher, P. (2011). Control of redox state and redox signaling by neural antioxidant systems. Antioxid. Redox Signal. *14*, 1449–1465.

Linker, R.A., Lee, D.H., Ryan, S., van Dam, A.M., Conrad, R., Bista, P., Zeng, W., Hronowsky, X., Buko, A., Chollate, S., et al. (2011). Fumaric acid esters exert neuroprotective effects in neuroinflammation via activation of the Nrf2 antioxidant pathway. Brain *134*, 678–692.

Liu, Z., Vuohelainen, V., Tarkka, M., Tenhunen, J., Lappalainen, R.S., Narkilahti, S., Paavonen, T., Oksala, N., Wu, Z., and Mennander, A. (2010). Glutamate release predicts ongoing myocardial ischemia of rat hearts. Scand. J. Clin. Lab. Invest. *70*, 217–224.

Lo, S.C., and Hannink, M. (2008). PGAM5 tethers a ternary complex containing Keap1 and Nrf2 to mitochondria. Exp. Cell Res. *314*, 1789–1803.

Melo, L.G., Agrawal, R., Zhang, L., Rezvani, M., Mangi, A.A., Ehsan, A., Griese, D.P., Dell'Acqua, G., Mann, M.J., Oyama, J., et al. (2002). Gene therapy strategy for long-term myocardial protection using adeno-associated virus-mediated delivery of heme oxygenase gene. Circulation *105*, 602–607.

Morioka, I., Wong, R.J., Abate, A., Vreman, H.J., Contag, C.H., and Stevenson, D.K. (2006). Systemic effects of orally-administered zinc and tin (IV) metalloporphyrins on heme oxygenase expression in mice. Pediatr. Res. *59*, 667–672.

Motohashi, H., and Yamamoto, M. (2004). Nrf2-Keap1 defines a physiologically important stress response mechanism. Trends Mol. Med. *10*, 549–557.

Mukherjee, S., Gangopadhyay, H., and Das, D.K. (2008). Broccoli: a unique vegetable that protects mammalian hearts through the redox cycling of the thioredoxin superfamily. J. Agric. Food Chem. *56*, 609–617.

Ooi, A., Wong, J.C., Petillo, D., Roossien, D., Perrier-Trudova, V., Whitten, D., Min, B.W., Tan, M.H., Zhang, Z., Yang, X.J., et al. (2011). An antioxidant response phenotype shared between hereditary and sporadic type 2 papillary renal cell carcinoma. Cancer Cell *20*, 511–523.

Penney, D.G., and Cascarano, J. (1970). Anaerobic rat heart. Effects of glucose and tricarboxylic acid-cycle metabolites on metabolism and physiological performance. Biochem. J. *118*, 221–227.

Peuhkurinen, K.J., Takala, T.E., Nuutinen, E.M., and Hassinen, I.E. (1983). Tricarboxylic acid cycle metabolites during ischemia in isolated perfused rat heart. Am. J. Physiol. *244*, H281–H288.

Piantadosi, C.A., Carraway, M.S., Babiker, A., and Suliman, H.B. (2008). Heme oxygenase-1 regulates cardiac mitochondrial biogenesis via Nrf2-mediated transcriptional control of nuclear respiratory factor-1. Circ. Res. *103*, 1232–1240.

Pollard, P.J., Spencer-Dene, B., Shukla, D., Howarth, K., Nye, E., El-Bahrawy, M., Deheragoda, M., Joannou, M., McDonald, S., Martin, A., et al. (2007). Targeted inactivation of fh1 causes proliferative renal cyst development and activation of the hypoxia pathway. Cancer Cell *11*, 311–319.

Rada, P., Rojo, A.I., Chowdhry, S., McMahon, M., Hayes, J.D., and Cuadrado, A. (2011). SCF/{beta}-TrCP promotes glycogen synthase kinase 3-dependent degradation of the Nrf2 transcription factor in a Keap1-independent manner. Mol. Cell. Biol. *31*, 1121–1133.

Rajasekaran, N.S., Connell, P., Christians, E.S., Yan, L.J., Taylor, R.P., Orosz, A., Zhang, X.Q., Stevenson, T.J., Peshock, R.M., Leopold, J.A., et al. (2007). Human alpha B-crystallin mutation causes oxido-reductive stress and protein aggregation cardiomyopathy in mice. Cell *130*, 427–439.

Rajasekaran, N.S., Varadharaj, S., Khanderao, G.D., Davidson, C.J., Kannan, S., Firpo, M.A., Zweier, J.L., and Benjamin, I.J. (2011). Sustained activation of nuclear erythroid 2-related factor 2/antioxidant response element signaling promotes reductive stress in the human mutant protein aggregation cardiomyopathy in mice. Antioxid. Redox Signal. *14*, 957–971.

Sanborn, T., Gavin, W., Berkowitz, S., Perille, T., and Lesch, M. (1979). Augmented conversion of aspartate and glutamate to succinate during anoxia in rabbit heart. Am. J. Physiol. *237*, H535–H541.

Sapieha, P., Sirinyan, M., Hamel, D., Zaniolo, K., Joyal, J.S., Cho, J.H., Honore, J.C., Kermorvant-Duchemin, E., Varma, D.R., Tremblay, S., et al. (2008). The succinate receptor GPR91 in neurons has a major role in retinal angiogenesis. Nat. Med. *14*, 1067–1076.

Schroeder, M.A., Cochlin, L.E., Heather, L.C., Clarke, K., Radda, G.K., and Tyler, D.J. (2008). In vivo assessment of pyruvate dehydrogenase flux in the heart using hyperpolarized carbon-13 magnetic resonance. Proc. Natl. Acad. Sci. USA *105*, 12051–12056.

Schroeder, M.A., Atherton, H.J., Ball, D.R., Cole, M.A., Heather, L.C., Griffin, J.L., Clarke, K., Radda, G.K., and Tyler, D.J. (2009). Real-time assessment of Krebs cycle metabolism using hyperpolarized 13C magnetic resonance spectroscopy. FASEB J. *23*, 2529–2538.

Shannon, P., Markiel, A., Ozier, O., Baliga, N.S., Wang, J.T., Ramage, D., Amin, N., Schwikowski, B., and Ideker, T. (2003). Cytoscape: a software environment for integrated models of biomolecular interaction networks. Genome Res. *13*, 2498–2504.

Smith, A.C., and Robinson, A.J. (2011). A metabolic model of the mitochondrion and its use in modelling diseases of the tricarboxylic acid cycle. BMC Syst. Biol. *5*, 102.

Soares, M.P., Lin, Y., Anrather, J., Csizmadia, E., Takigami, K., Sato, K., Grey, S.T., Colvin, R.B., Choi, A.M., Poss, K.D., and Bach, F.H. (1998). Expression of heme oxygenase-1 can determine cardiac xenograft survival. Nat. Med. *4*, 1073–1077.

Spencer, S.R., Wilczak, C.A., and Talalay, P. (1990). Induction of glutathione transferases and NAD(P)H:quinone reductase by fumaric acid derivatives in rodent cells and tissues. Cancer Res. *50*, 7871–7875.

Sussan, T.E., Rangasamy, T., Blake, D.J., Malhotra, D., El-Haddad, H., Bedja, D., Yates, M.S., Kombairaju, P., Yamamoto, M., Liby, K.T., et al. (2009). Targeting Nrf2 with the triterpenoid CDDO-imidazolide attenuates cigarette smoke-induced emphysema and cardiac dysfunction in mice. Proc. Natl. Acad. Sci. USA *106*, 250–255.

Taegtmeyer, H. (1978). Metabolic responses to cardiac hypoxia. Increased production of succinate by rabbit papillary muscles. Circ. Res. *43*, 808–815.

Taguchi, K., Maher, J.M., Suzuki, T., Kawatani, Y., Motohashi, H., and Yamamoto, M. (2010). Genetic analysis of cytoprotective functions supported by graded expression of Keap1. Mol. Cell. Biol. *30*, 3016–3026.

Taguchi, K., Motohashi, H., and Yamamoto, M. (2011). Molecular mechanisms of the Keap1-Nrf2 pathway in stress response and cancer evolution. Genes Cells *16*, 123–140.

Van Wylen, D.G. (1994). Effect of ischemic preconditioning on interstitial purine metabolite and lactate accumulation during myocardial ischemia. Circulation *89*, 2283–2289.

Vincent, G., Comte, B., Poirier, M., and Rosiers, C.D. (2000). Citrate release by perfused rat hearts: a window on mitochondrial cataplerosis. Am. J. Physiol. Endocrinol. Metab. *278*, E846–E856.

Vreman, H.J., Lee, O.K., and Stevenson, D.K. (1991). In vitro and in vivo characteristics of a heme oxygenase inhibitor: ZnBG. Am. J. Med. Sci. *302*, 335–341.

Wiesner, R.J., Rosen, P., and Grieshaber, M.K. (1988). Pathways of succinate formation and their contribution to improvement of cardiac function in the hypoxic rat heart. Biochem. Med. Metab. Biol. *40*, 19–34.

Wikstrom, B.G., Ronquist, G., and Waldenstrom, A. (1995). Dynamics of myocardial metabolism in the preconditioned porcine heart studied using continuous microdialysis. Eur. Heart J. *16*, 563–569.

Willems, L., Zatta, A., Holmgren, K., Ashton, K.J., and Headrick, J.P. (2005). Age-related changes in ischemic tolerance in male and female mouse hearts. J. Mol. Cell. Cardiol. *38*, 245–256.

Witney, T.H., Kettunen, M.I., and Brindle, K.M. (2011). Kinetic modeling of hyperpolarized 13C label exchange between pyruvate and lactate in tumor cells. J. Biol. Chem. *286*, 24572–24580.

Yellon, D.M., and Hausenloy, D.J. (2007). Myocardial reperfusion injury. N. Engl. J. Med. *357*, 1121–1135.

Yet, S.F., Tian, R., Layne, M.D., Wang, Z.Y., Maemura, K., Solovyeva, M., Ith, B., Melo, L.G., Zhang, L., Ingwall, J.S., et al. (2001). Cardiac-specific expression of heme oxygenase-1 protects against ischemia and reperfusion injury in transgenic mice. Circ. Res. *89*, 168–173.

Zhang, W., Contag, P.R., Hardy, J., Zhao, H., Vreman, H.J., Hajdena-Dawson, M., Wong, R.J., Stevenson, D.K., and Contag, C.H. (2002). Selection of potential therapeutics based on in vivo spatiotemporal transcription patterns of heme oxygenase-1. J. Mol. Med. (Berl.) *80*, 655–664.

Zhang, Y., Sano, M., Shinmura, K., Tamaki, K., Katsumata, Y., Matsuhashi, T., Morizane, S., Ito, H., Hishiki, T., Endo, J., et al. (2010). 4-hydroxy-2-nonenal protects against cardiac ischemia-reperfusion injury via the Nrf2-dependent pathway. J. Mol. Cell. Cardiol. *49*, 576–586.